https://doi.org/10.1590/jatm.v13.1185 ORIGINAL PAPER

Study of Flow Field Inside a Can Combustor for Micro Gas Turbine Engine Under Nonreacting Flow Conditions

Kirubakaran Vijayakumar[1], David Bhatt[1,*]

1. Vel Tech Rangarajan Dr. Sagunthala R&D Institute of Science and Technology – Department of Aeronautical Engineering– Chennai/Tamil Nadu – India

***Corresponding author:** davidbhatt@gmail.com

ABSTRACT

Generally, micro gas turbines are in the range of 15 to 300 kW. However, recent applications in unmanned aerial vehicles (UAVs) and polygeneration require a small micro gas turbine. So, here a small swirl combustor designed for micro gas turbine engine of capacity less than 1 kW is analyzed under nonreacting flow conditions. Simulations have been carried out to study the flow field inside the can combustor. Flow field characteristics, like velocity, path lines, turbulent intensity and total pressure loss are studied. The total pressure loss across the combustor is also measured experimentally and compared with that of simulation results. Good agreement is achieved between experimental and numerical results. The combustor total pressure drop was found to be negligible in the range of 0.002 to 0.06% at an inlet velocity ranges from 1.7 to 10.19 m/s. Flow pattern indicates a strong swirling pattern and strong interaction between the secondary air entrainment inside the flame tube.

Keywords: Combustor; Combustion chamber; Gas turbine engines; Turbulent flow.

INTRODUCTION

Due to the requirement of high rpm of turbo machinery for the sake of efficiency, most of the micro gas turbine was developed for a power in range of 15 to 300 kW (Nascimento *et al.* 2013). However, recent need in combined heat and power generation (CHP) at remote places, distributed generation is economically viable and reduces transmission losses (Pilavachi 2002). Due to this, interest has been arisen in developing micro gas turbine engines for low power. Recent advances in the development of recuperate have enabled to increase the net electrical efficiency of MGT from 12 to 17% (Xiao *et al.* 2017). Another potential application of this is for power generation to run mobile tower at remote places, which typically require around 12 kW. Besides, this technology also favors poly generation and enhance overall efficiency by utilization of waste heat (Rahman and Malmquist 2016). When compared with other technologies for small scale power generation, they offer numerous advantages which include high-grade heat and lower emission levels, compact size, reduced noise and vibrations, easy operations and installations. Gas turbine technology is highly suitable for power generation from biofuels, as it offers good flexibility to be used with a variety of fuels with

Received: Feb. 3, 2020 | **Accepted:** Aug. 6, 2020
Peer Review History: Double Blind Peer Review
Section Editor: T. John Tharakan

negligible changes in the components (Oppong *et al.* 2015; Fuchs *et al.* 2016). Thus, new biofuels/biogas can be easily fed to these engines; one such engine on biogas has been tried.

From the literature, the nonreacting flow analysis in the gas turbine combustor was carried out by numerous researchers (Reddy and Ganesan 2004; Dzida and Kosowski 1989; Karuppannan *et al.* 2018). Among them, a notable work has been carried out (Reddy and Ganesan 2004), wherein detailed 3D flow has been simulated inside an annular combustor using a 20-degree sector model for analysis. The k-ε renormalization group (RNG) model was used to model turbulence. The total pressure loss of the combustor varied from 4.41 to 9.87% for a given set of input velocity, 158.8 to 238.20 m/s. The major challenge in the design of diffuser system for gas turbine engines is that the maximum static pressure recovery should be achieved in the shortest possible length with minimum pressure loss (Lefebvre and Ballal 2010). Shankar *et al.* (2019) studied the characteristics of a coflowing jet with varying lip thickness, the study shows that the total pressure decay increases with increase in lip thickness of coflowing jet. Karuppannan *et al.* (2018) study of the flow behavior in the annular diffuser has been analyzed by simulating realistic downstream combustor liner and transition duct geometry. The minimal total pressure loss of their pre-diffuser is experienced by 0.13%. In the study by Crocker *et al.* (1999) on computational fluid dynamics (CFD) modeling of gas turbine combustor from compressor exit to turbine inlet, the detailed flow analysis was carried out for liner and wall temperature predictions. Hall *et al.* (2014) simulated a nonreacting flow in a swirl combustor. They have noted that nonuniform combustor outlet flows have been demonstrated to have a significant impact on the first and second stage turbine aero thermal performance.

Most of the previous studies are on a large-scale combustor employed in high power gas turbines. However, the large-scale combustors cannot be scaled down as it is due to unscalable parameters, such as characteristic combustion time (Van den Braembussche 2005). Hence, modification in the combustor design is required for making the combustor compact e.g., reverse flow combustor (Krieger *et al.* 2012). On the other hand, the volume of combustor is a scalable parameter. Other factors that need to be considered are the avoidance of hot spots to ensure durability and geometrical restrictions related to manufacturing of miniaturized components. In the design considered in this paper, a strong recirculation zone is created inside the combustion liner by restricting the bypass air to pass through the dilution holes only.

The purpose of the present study is to investigate a nonreacting flow inside the newly designed 3 kW thermal power swirl stabilized micro gas turbine combustor. This will be useful for building a micro gas turbine engine suitable for standalone off-grid power generator. It is also envisioned to be used for a long endurance UAV.

COMBUSTOR GEOMETRY

A microcombustor with capacity of 3 kW was designed by considering the design principles mentioned in standard textbooks (Lefebvre and Ballal 2010; Mattingly 2005; Hill and Peterson 2014). A sectional view of the combustor is shown in Fig. 1. This combustor is composed of diffuser, snout, swirler, flame tube and outer casing. The conical diffuser has an angle of divergence of 24.2 degrees, whereas the snout has a divergence angle of 24.8 degrees. An axial swirler with 8 number of flat vanes are arranged at 45 degrees to the axis and inclined to radial direction by 25 degrees. Length of the swirler is taken to be 30 mm. The swirl number is estimated to be 0.75. The flame tube has 265 mm length and 46 mm diameter, its primary zone has 88 numbers of 2 mm holes arranged in 4 rows, secondary zone has 60 numbers of 3 mm holes arranged in 4 rows and dilution zone has 24 numbers of 2 mm holes arranged in 3 rows. The detail distribution of holes is given in Table 1. The outer annulus has 300 mm of length with 72 and 44 mm of inlet and outlet diameter. The overall thickness of can combustor is maintained as 2 mm thickness.

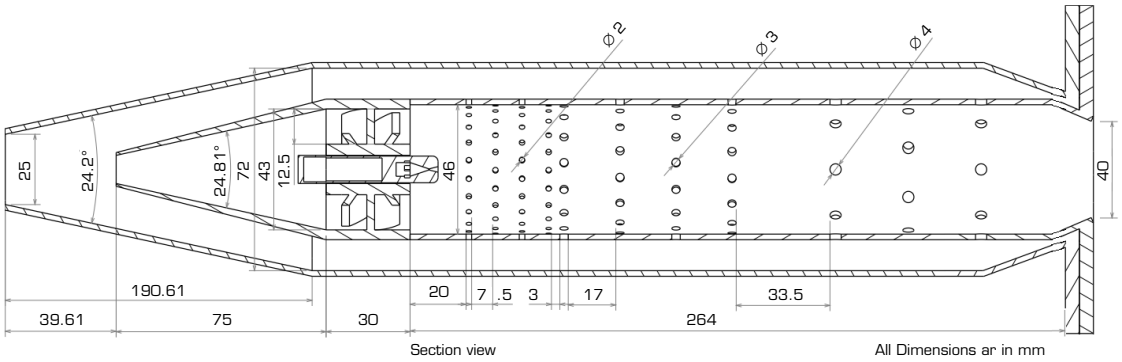

Figure 1. Dimension details of can combustor.

Table 1. Dimensional details of the flame tube.

S.No	Description	Primary port	Secondary port	Dilution port
1	Hole Diameter (mm)	2	3	4
2	Number of rows	4	4	3
3	Row Spacing (mm)	8	20	26
4	Angle between holes (deg)	18	24	45
5	Number of holes in each row	22	15	8
6	Total number of holes	88	60	24
7	Area of flow passage (mm^2)	276.32	423.9	301.44

The diffuser expands the flow slightly until it reaches snout, where it splits into two streams. One stream enters and expands in the snout. This enters the swirler, where a strong swirling motion of air is generated. The swirler is designed so that the fuel enters in the flame tube through the center of the swirler. This helps to mix the reactants and stabilize the flame near to the swirler upon ignition. This annulus flow, which was bypassed at the snout, enters the flame tube through different ports provided on the flame tube. These ports are distributed on the liner by 3 different zones viz. primary, secondary and dilution zone. Excess combustion air required for complete combustion enters through primary and secondary zones. This distribution helps in distributed combustion, thereby reducing the instability. Finally, the air entering through the dilution zones helps to lower the burnt gas temperature up to a safe level for the turbine. Here the bypass air enters only through these holes.

As a primary phase of combustor flow characterization, the total pressure drop across this combustor in a nonreacting mode was experimentally and numerically studied. To perform the stand-alone combustor test, the compressed air from reciprocating compressor is passed through the prediffuser.

EXPERIMENTAL STUDY

To test the combustor for flame stabilization and performance, an experimental set up was built. As far as the nonreacting flow characterization is considered, the pressure drop across the combustor is measured. Figure 2 shows the schematic diagram of the setup used to measure the pressure drop.

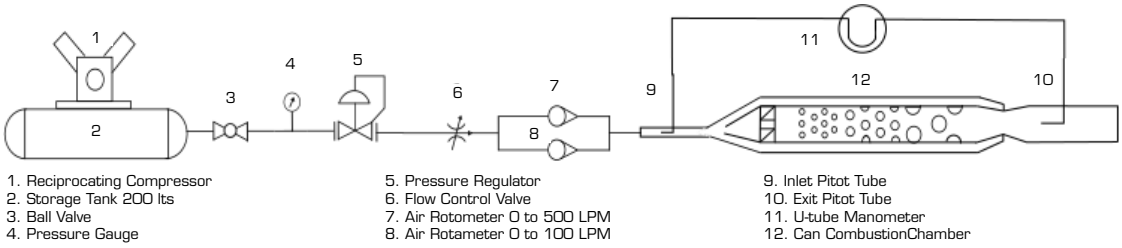

Figure 2. Can combustor cold-flow experimental setup layout.

Air is compressed up to 5 bar using a dual-stage reciprocating compressor. The pressure of the compressed air is regulated and the flow rate is controlled using a flow control valve. Controlled air is passed through the inlet of the combustor. The flow rate is measured with the help of two rotameters (7&8) connected in parallel. The rotameter-7 is used for coarse control of air mass flow rate from 0 to 500 LPM with 10 LPM as a least count (make: Wieser; measurement error within 0.2 - 20 LPM is ± 4%) and the rotameter-8 is used for fine control of air mass flow rate from 0 to 100 LPM with 1 LPM as a least count (make: Wieser; measurement error within 0.04 - 4 LPM is ± 4%). The net mass flow of air passing through the combustor is the sum of two rotameters flow. The two pitot tubes are used to measure the total pressure, one at inlet and other at the outlet of the combustor. A U-tube water manometer is connected to these two pitot tubes to read the difference of total pressure directly. The readings were taken after a minute for each case in order to get the stabilized results. To ensure the repeatability of experimental predicted values, each test case was conducted three times and the average of three cases is taken as final reading for each case.

NUMERICAL STUDY

A numerical simulation was performed to predict the detailed flow field characteristics of the combustor for 1:1 scale as similar to experimental study for the inlet velocity ranges from 1.70 to 10.19 m/s. Since this combustor is designed to stabilize the flame using swirling flow, the flow inside is assumed to be swirling. Swirling motion is essentially 3-dimensional; however, there is some symmetry in the angular direction. Thus, to simplify the problem, it is modeled by taking only a sector of a suitable angle. In this case, since there are 8 swirling vanes, a 45-degree sector would be sufficient. However, the full view of the swirling vanes is in a split view. Hence, to avoid this, the 90-degree sector was taken for analysis. The combustor flame tube wall thickness was assumed as zero to minimize the complexities arising due to small vortices.

It is essential for the purposes of the present study to check the flow characteristics with the help of Reynolds number. To estimate the Reynolds number, inlet velocity is used and flame tube diameter is used as length scale. Reynolds number for the combustor inlet flow velocity from 1.70 to 10.19 m/s, comes out to be in range of 2,874 to 17,243. These values indicate that the flow inside the combustor is turbulent in nature for the entire test range. Apart from this, as the combustor inlet flow is supplied form a compressor, typically a radial compressor in case of microturbine, the inlet flow is itself turbulent. This radial compressor typically runs for very high rpm, so the flow at exit of the compressor is assumed to be turbulent. Hence, it is necessary to choose a turbulent model to study the flow field inside the combustion chamber.

Steady state RANS simulation is carried out using k-ε RNG turbulence model (Reddy and Ganesan 2004). The combustor inlet is specified as a velocity boundary. The outlet of the geometry is specified as a pressure outlet. The inlet and outlet of snout, swirler, primary ports, secondary ports and dilution ports are specified as an interior. The sectional plane of the sector model is specified as periodic boundary. The remaining faces of combustor model are specified as a wall. The computational domain taken in the present study is shown in Fig. 3.

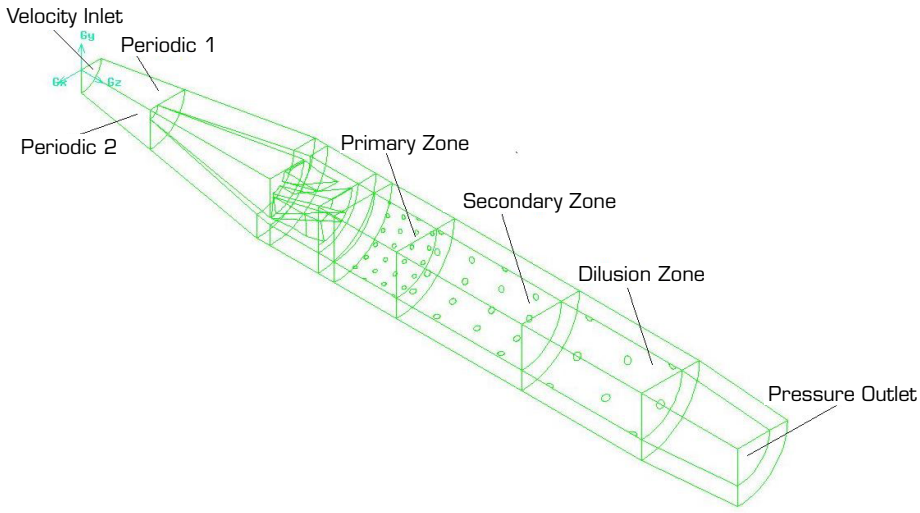

Figure 3. Computational domain: 90-degree sector of can combustor.

Grid sensitivity

The unstructured grid has been employed due to the complexity of combustor geometry. The grid sensitivity study is carried out for four different grid sizes. A mass weight average of total pressure is compared with Grid-D. The results were obtained numerically at 10.19 m/s inlet velocity, as shown in Table 2.

Table 2. Pressure loss comparisons for various grid sizes (10.19 m/s inlet velocity case).

Type	Grid type	Grid size (mm)	Elements	Differential pressure head (Pa)	Percentage difference (%)
Grid-A	Tetrahedral	1	2018026	51.898551	4
Grid-B(*)	Tetrahedral	0.9	2787636	48.808857	2
Grid-C	Tetrahedral	0.8	4009738	48.367445	2
Grid-D	Tetrahedral	0.7	5942049	46.06354	-

As seen from Table 2, almost similar results were obtained with Grid-B and Grid-C. Alternately, the center line velocity along the combustor dimensionless length for different grids (Fig. 4) is also considered. The combustor length was nondimensionalized with flame tube diameter. From the plot, its seen that the velocity profile matches closely for all grids considered. Hence, considering the optimality, Grid-B is adopted in the study.

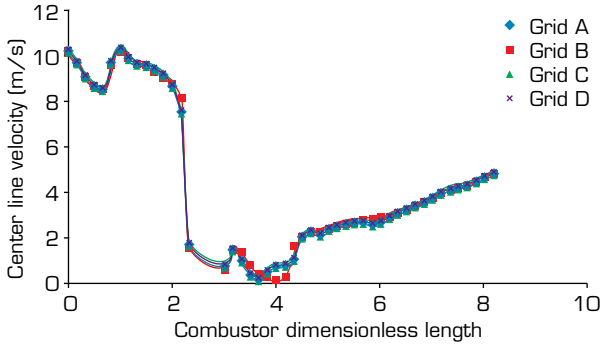

Figure 4. Center line velocity for different grid sizes at 10.19 m/s inlet velocity.

VALIDATION OF NUMERICAL RESULTS

Preliminary validation of numerical results is done by measuring the pressure loss (ΔP_{sw}) across the swirler and comparing with analytical expressions. The mass flow rate ($\dot{m}_{sw}$) of air passing through the swirler concerning its pressure loss is given by the following analytical equation Eq. 1 (Lefebvre and Ballal 2010).

$$\dot{m}_{sw} = \left\{ \frac{2\rho_3 \Delta P_{sw}}{K_{sw}\left[(\sec\theta / A_{sw})^2 - 1/A_L^2\right]} \right\}^{0.5} \tag{1}$$

where the swirler area (A_{sw}) is calculated by Eq. 2:

$$A_{sw} = (\pi / 4)(D^2 - D_h^2) - 0.5 n_v t_v (D - D_h) \tag{2}$$

From the relation above, the pressure loss across the swirler can be calculated and compared with numerical results for a range of inlet velocities considered in this study. Figure 5 shows the pressure loss with respect to dimensionless mass flow.

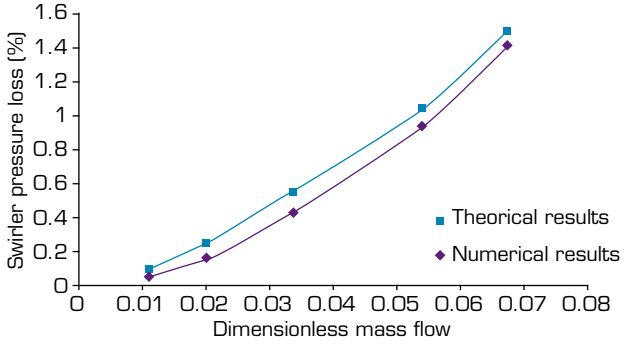

Figure 5. Swirler pressure loss for various dimensionless mass flow rates.

The mass flow rate of air can be nondimensionalized by the relation seen in Eq. 3 (Dixon and Hall 2010).

$$Q = \frac{\dot{m}_a \sqrt{C_P T_{01}}}{A_I P_{01}} \tag{3}$$

where Q is the dimensionless mass flow rate of air, $\dot{m}_a$ is the combustor inlet mass flow rate, C_p is the specific heat of air, T_{01} is the combustor inlet temperature, A_I combustor inlet area and P_{01} is the combustor inlet pressure. The theoretical prediction of pressure loss across the swirler shows good agreement with numerical predictions.

RESULTS AND DISCUSSION

The flow field inside a can combustor has been analyzed for a 90-degree sector model under nonreacting flow conditions. Except for flame tube wall thickness, the other blockages in geometry like snout wall, swirler wall and fuel injector were included

in the analysis. The flow filed and performance characteristics of the combustor for nonreacting flow conditions with inlet velocity ranges from 1.7 to 10.19 m/s with corresponding Reynolds number of 2,874 to 17,243 were analyzed.

To understand the overall distribution of airflow inside the various parts of the combustor, the amount of air passing through was calculated from the numerical results and is shown in Fig. 6. It can be seen that 20% of incoming air passes through the swirler through the snout. Remaining 80% entrains into the combustion chamber through the holes on the flame tube in three stages: 15% of this enters at primary zone, 20% at the secondary zone and remaining 45% enters at the dilution zone. It is also observed that this distribution doesn't change significantly for the range of inlet velocities considered here.

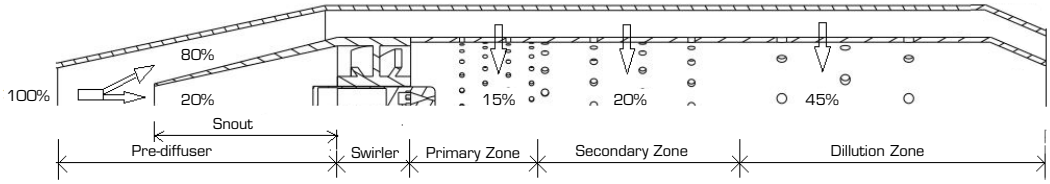

Figure 6. Combustor mean mass flow distribution for the velocity range 1.7 to 10.19 m/s.

Flow pattern inside the combustor

To understand the flow pattern inside the combustor, it is necessary to look at the velocity distribution shown in Fig.7. This plot shows the reconstructed velocity contour along the length of the combustor on the symmetric plane of the 90-degree sector combustor. As the compressed air enters the diffuser, the flow decelerates due to area enlargement. Further, when the flow reaches the snout, the amount of air entering the snout (core flow) accelerates and further decelerates due to area enlargement. Alternately, the secondary flow also decelerates because of constriction caused due to liner and blockage at the exit. When the core flow passes through swirler, swirling motion of air is seen in Fig. 8. The core flow turns by the swirl angle and emerges out of the swirler in the form of jets. A strong recirculation zone is also seen in the central core. As the secondary flow entrainment from the primary zone starts, the recirculation zone decays and its located between the swirler exit and the primary zone entry. Since the flow in the annular region is blocked at the exit, all flow passes through the primary, secondary and dilution zone ports in the liner. This causes the velocity of entrainment to be much higher than the central flow. The velocity of entrainment is so high that it creates a strong vortex, as seen from the vector plot along the cross-section A-A at z = 3.36 (Fig. 7). This rotational flow would be useful in stabilizing the flame even at ultra-lean mixtures. Further downstream, as the entrainment from subsequent ports increases the net mass flow, which results in increase in velocity.

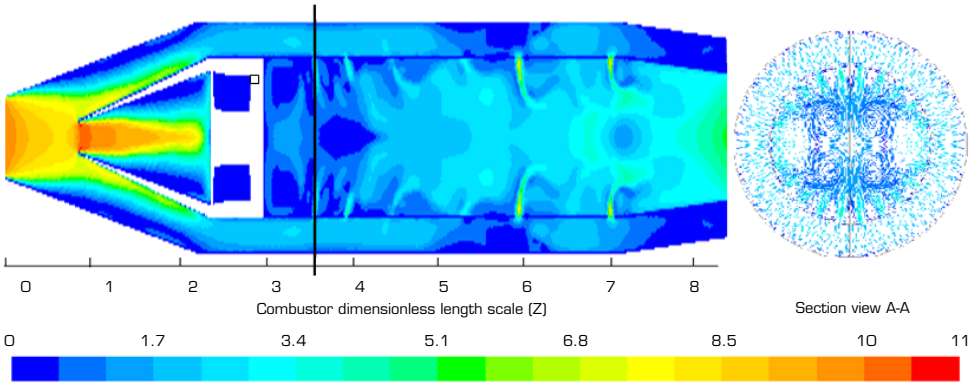

Figure 7. Contours of velocity magnitude for inlet velocity of 10.19 m/s case.

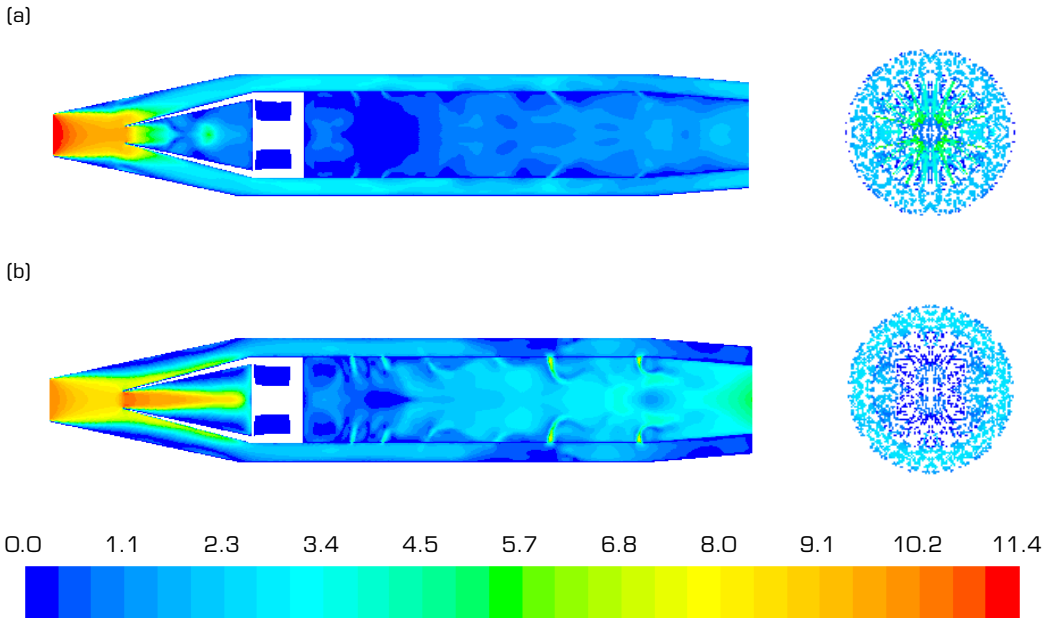

Figure 8. (a) and (b) show the velocity contour and vector plot for fully open and closed annulus exit combustor configrations.

Annulus flow study

Generally for conventional gas turbine combustors, the bypass flow exits the combustor through the annular region between the linear and the casing. However, in this case, the exit passage is closed to enhance the flame stabilization. In order to understand the flow changes, a simulation was carried for both cases:

- Open annulus configuration in which the bypass flow also exits through the opening at the end of the combustor;
- A fully closed annulus flows configuration, wherein the bypass flow through the annulus completely passes through the holes provide in the liner.

The velocity contours and vector plot for both configurations are shown in Fig. 8. As seen from the figure, the annulus flow plays a major role in primary, secondary and dilution jet penetrations.

In case of closed annular flow, the blockage of annulus exit flow give rise to increase in back pressure, which allows more core flow and less annulus flow, resulting in strong recirculation zone post the swirler. Further, the kinetic energy iof the entraining jets is much higher than that of the open confifuration. Thus, a deeper jet penetration is observed. All this would help in good mixing of fuel and air near the swirler and also aid in flame stabilization, even at low equivalence ratio.

On the other hand, the pressure drop for closed configuation experiences higher pressure drop (0.06%) when compared to open type (0.02%). However, this can be tolerable for application in microgas turbine, where flame stabilization matters more than efficiency. Another problem envisizged would be decreased heat loss. However, as in the case of microcombustor, the surface to volunme ratio is higher, the cooling of linear can easiliy be achieved by flow of cooling air on the external surface of the combustor casing.

Variation of flow for varying inlet velocity

The study above for flow field is carried out for cases with different velocities of less than 10 m/s. However, some representative behaviors viz. velocity and turbulent intensity are presented to understand the change for inlet velocities less than 10 m/s in the range considered in this study.

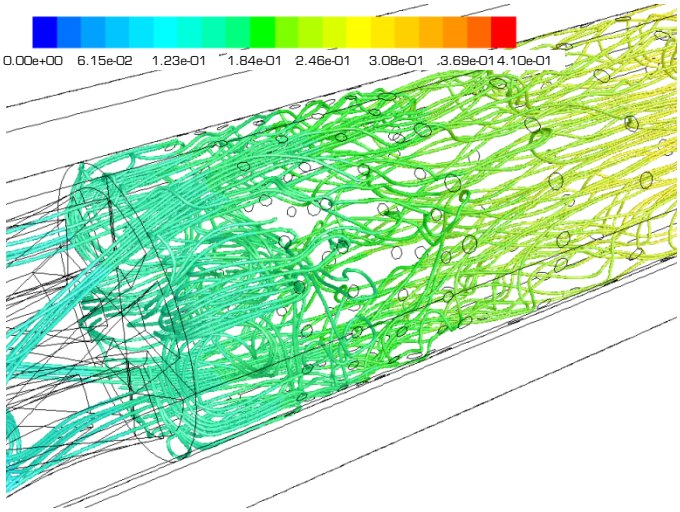

Figure 9. Path lines inside the swirler and flame tube for inlet velocity of 10.19 m/s (color indicate axial distance from the combustor inlet in meter).

Centre line velocity variation along the combustor

Figure 10 shows the center line velocity distribution along the combustor for various values of inlet velocities. When the flow enters the combustor through pre-diffuser, center line velocity is decreased by a small amount. However, as it enters the snout, velocity begins to increase rapidly, then decreases due to expansion of area in the snout. The local acceleration at the center line is due to shear at the snout wall which decelerates the flow near the wall and accelerates in the center. Since the central part of flow is blocked in this work, the center line velocity is seen to reduce to very low value. Past the swirler, a small rise in velocity is indicative of central recirculating zone, as seen earlier, which decays as entrainment increases. Further upon entrainment, the swirl starts decaying and flow tends to be uniform along the cross-section. So, the center line velocity increases due to an increase in the entrainment of air from the secondary and dilution ports.

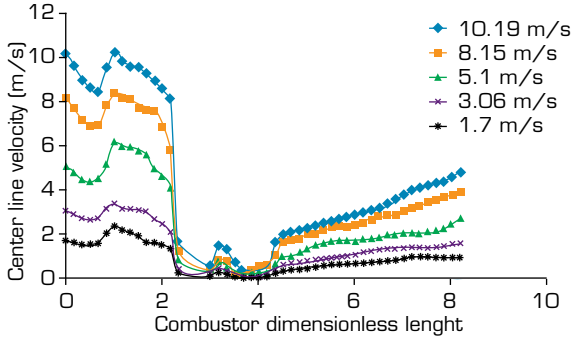

Figure 10. Center line velocity for various inlet velocities cases.

Centre line turbulent intensity variation along the combustor

Figure 11 shows variation of turbulent intensity along the length of the combustor. It is seen that the turbulent intensity is almost constant for an initial part in diffuser section. As it reaches the snout, it starts to rise steeply due to increase in shear forces at the entrance of snout. This trend continues until it reaches peak intensity. This phenomenon occurs since as the flow enters the swirler it encounters more blockages, which may be due to increased vertical flow and constriction at the entrance of the swirler. Further, as the flow passes through the swirler, the turbulent intensity drops down. This may be due to the effect of shear inside the passage of vanes, which dissipates the kinetic energy. Additionally, the turbulent intensity remains almost constant.

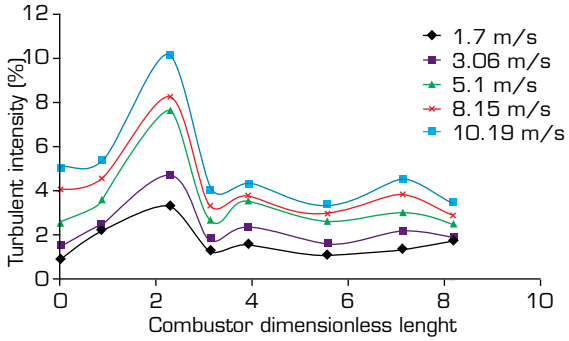

Figure 11. Turbulent intensity along the centerline for various inlet velocities.

Combustor outlet velocity

Figure 12 shows the combustor outlet velocity to inlet velocity. A linear trend was observed for combustor outlet velocity variation with respect to inlet velocity. A similar trend was observed from a previous work on large gas turbine combustor for the velocity ranges from 158.8 to 238.20 m/s (Reddy and Ganesan 2004). It is interesting to observe similar trend in micro gas turbine combustor for the velocity ranges from 1.7 to 10.19 m/s.

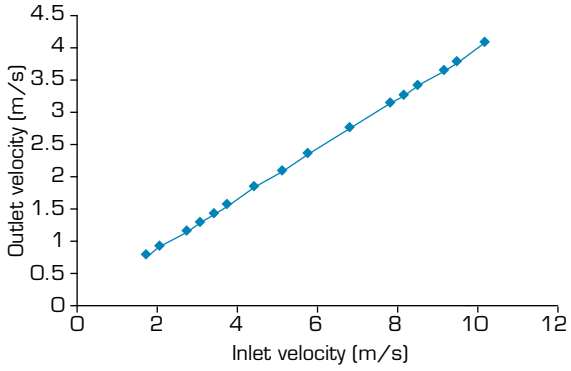

Figure 12. Combustor outlet velocity variation for different inlet velocities.

Combustor pressure loss

Total pressure drop, which is a good measure of energy dissipated in the combustor, is calculated from both experiments and numerical simulation. The experimental and numerical results of total pressure loss for various nondimensional mass flow rates are shown in Fig.13. As seen from Fig.13, the pressure loss increases almost linearly with inlet mass flow from 0.002 to 0.06% as velocity varies from 1.7 to 10.19 m/s. The good agreement found between experimental and numerical results.

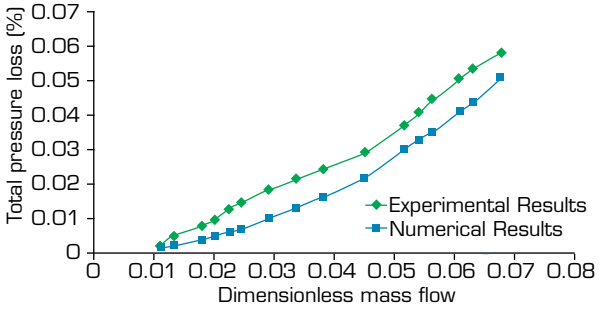

Figure 13. Combustor total pressure loss for various dimensionless mass flows.

CONCLUSIONS

The typical nonreacting flow inside the micro can-type combustor is studied experimentally, as well as numerically. A swirler creates a strong recirculation zone due to the effect of radial pressure and the interaction of opposing primary jets. This would create a strong mixing of air and fuel and achieve distributed flame region inside the combustor. The combustor total pressure drop was found to be negligible in the range of 0.002 to 0.06% at an inlet velocity ranging from 1.7 to 10.19 m/s. As the inlet mass flow is increased, the total pressure loss across the combustor also increases. Because of combustor inlet to outlet area variation, the combustor exit velocity is seen to be reduced to 40%.

This work can be extended to include the reactive flow analysis. This will help to predict the lean and rich blowout of combustor. It is also planned to verify it in experiments, in order to establish flame stability map of the combustor.

AUTHOR'S CONTRIBUTION

Conceptualization: Bhatt DS; **Methodology:** Bhatt DS; **Investigation:** Vijaykumar K; **Validation:** Vijaykumar K; **Writing – Original Draft:** Vijaykumar K; **Writing – Review and Editing:** Bhatt DS and Vijaykumar K; **Supervision:** Bhatt DS.

DATA AVAILABILITY STATEMENT

The data will be available upon request.

FUNDING

Not applicable.

ACKNOWLEDGEMENT

The authors thank Prof. A. T. Ravichandran, Head, Department of Mechanical Engineering, VelTech Rangarajan Dr. Sagunthala R&D Institute of Science and Technology for permitting to conduct experiments. The authors also thank staff member Mr. Satish for his support to conduct experiments.

REFERENCES

Crocker DS, Nickolaus D, Smith CE (1999) CFD Modeling of a gas turbine combustor from compressor exit to turbine inlet. J Eng Gas Turbines Powe 121(1):89-95. https://doi.org/10.1115/1.2816318

Dixon SL, Hall CA (2010) Fluid mechanics and thermodynamics of turbo-machine. Oxford: Butterworth-Helnemann. https://doi.org/10.1016/C2009-0-20205-4

Dzida M, Kosowski K (1989) Experimental investigations of pressure drop in the combustion chamber of gas turbine. Paper presented ASME 1989 International Gas Turbine and Aeroengine Congress and Exposition. ASME; Toronto, Ontario,

Canada. https://doi.org/10.1115/89-GT-247

Fuchs F, Meidinger V, Neuburger N, Reiter T, Zündel M, Hupfer A (2016) Challenges in designing very small jet engines - fuel distribution and atomization. Paper presented 16th International Symposium on Transport Phenomena and Dynamics of Rotating Machinery. HAL; Honolulu, Hawaii, United States. [accessed Sep 3 2019]. https://hal.archives-ouvertes.fr/hal-01891309/document

Hall BF, Chana KS, Povey T (2014) Design of a nonreacting combustor simulator with swirl and temperature distortion with experimental validation. J Eng Gas Turbines Power 136(8):081501. https://doi.org/10.1115/1.4026809

Hill PG, Peterson CR (2014) Mechanics and thermodynamics of propulsion. Upper Saddle River: Prentice Hall.

Karuppannan S, Sondur VM, Sivaramakrishna G, Navindgi RD, Muthuveerappan N (2018) CFD Analyses of Combustor-diffuser system of marine gas turbine engine. Paper presented ASME 2017 Gas Turbine India Conference. ASME; Bangalore, India. https://doi.org/10.1115/GTINDIA2017-4739

Krieger GC, Campos APV, Sacomano Filho FL, Souza RC (2012) A Swirler stabilized combustion chamber for a micro-gas turbine fuelled with natural gas. J Braz Soc Mech Sci & Eng 34(4):441-449. https://doi.org/10.1590/S1678-58782012000400004

Lefebvre HA, Ballal DR (2010) Gas turbine combustion: Alternative fuels and emissions. Boca Raton: CRC Press. https://doi.org/10.1201/9781420086058

Mattingly JD (2005) Elements of Gas Turbine Propulsion. Reston: AIAA.

Nascimento MAR, Rodrigues LD, Santos EC, Gomes EEB, Dias FLG, Velásques EIG, Carrillo RAM (2013) Micro gas turbine engine: a review. In: Benini E editor. Progress in Gas Turbine Perform. London: IntechOpen. https://doi.org/10.5772/54444

Oppong F, van der Spuy S, von Backström T and Diaby AL (2015) An overview of micro gas turbine engine performance investigation. R&D J 31:35-41.

Pilavachi PA (2002) Mini- and micro-gas turbines for combined heat and power. Appl Therm Eng 22(18):2003-2014. https://doi.org/10.1016/S1359-4311(02)00132-1

Rahman M, Malmquist A (2016) Modeling and simulation of an externally fired micro-gas turbine for standalone polygeneration application. J Eng Gas Turbines Power 138(11):112301. https://doi.org/10.1115/1.4033510

Reddy GA, Ganesan, V (2004) Non-reacting flow analysis from combustor inlet to outlet using computational fluid dynamics code. Defence Sci J 54(4):455-467. https://doi.org/10.14429/dsj.54.2059

Shankar RN, Bennett SK, Raja ND, Kumar KS (2019) Characteristics of a co-flowing jet with varying lip thickness and constant velocity ratio. Aircr Eng Aerosp Technol 92(4):633-644. https://doi.org/10.1108/AEAT-05-2019-0104

Van den Braembussche RA (2005) Micro gas turbines — A short survey of design problems. In: Micro Gas Turbines. Neuilly-sur-Seine: RTO.

Xiao G, Yang T, Liu H, Ni D, Ferrari ML, Li M, Luo Z, Cen K, Ni M (2017) Recuperators for micro gas turbines: A review. Appl Energy 197:83-99. https://doi.org/10.1016/j.apenergy.2017.03.095